

# Geophysical Research Letters

## RESEARCH LETTER

10.1029/2019GL085399

### Key Points:

- Previous estimates of Hermean flux transfer event (FTE) content make implicit assumptions about FTE structure
- Removing these assumptions results in estimates of FTE flux content at Mercury which are up to 5 times greater
- FTEs may provide more than enough flux transport to drive Mercury's substorm cycle, contrary to previous reports

### Correspondence to:

R. C. Fear,  
R.C.Fear@soton.ac.uk

### Citation:

Fear, R. C., Coxon, J. C., & Jackman, C. M. (2019). The contribution of flux transfer events to Mercury's Dungey cycle. *Geophysical Research Letters*, 46, 14,239–14,246. <https://doi.org/10.1029/2019GL085399>

Received 19 SEP 2019

Accepted 2 DEC 2019

Accepted article online 4 DEC 2019

Published online 23 DEC 2019

## The Contribution of Flux Transfer Events to Mercury's Dungey Cycle

R. C. Fear<sup>1</sup>, J. C. Coxon<sup>1</sup>, and C. M. Jackman<sup>1</sup>

<sup>1</sup>School of Physics and Astronomy, University of Southampton, Southampton, UK

**Abstract** Bursty dayside reconnection plays a proportionally larger role in the driving of Mercury's magnetosphere than it does at Earth. Individual bursts of reconnection, called flux transfer events (FTEs), are thought to open up to 5% of Mercury's polar cap; coupled with the much higher repetition rate of FTEs at Mercury and the short Dungey cycle timescale, this makes FTEs the major driver of Mercury's magnetosphere. However, comparison between spacecraft and ionospheric observations at Earth suggests that the terrestrial contribution of FTEs may have been severely underestimated, by making implicit assumptions about FTE structure. In this study, we consider the implications of removing these assumptions at Mercury; by considering FTE mechanisms based on longer reconnection lines, we find that the contribution of FTEs to Mercury's Dungey cycle could be 5 times greater than previously thought and that FTEs may be able to provide sufficient flux transport to drive Mercury's substorm cycle.

**Plain Language Summary** Planets with a magnetic field carve out a cavity, or “magnetosphere” in the solar wind. The magnetosphere of Mercury, like that of Earth, is driven by a process called “magnetic reconnection”, in which magnetic fields from the Sun and the planet interconnect. Reconnection at Mercury (and Earth) occurs in bursts called “flux transfer events”, but the contribution of such events to the global dynamics of the magnetosphere has been debated. Individual bursts of reconnection are already thought to be much more significant at Mercury than Earth (relative to the sizes of these two magnetospheres), but we argue that the contribution made by individual events at Mercury has nonetheless been underestimated, potentially by a factor of 5. At an upper limit, a handful of individual reconnection events may be capable of entirely refreshing the “open” part of Mercury's magnetosphere, and bursty reconnection may be capable of providing enough magnetic flux to drive the dynamics of Mercury's magnetosphere in their entirety.

## 1. Introduction

Mariner 10 observations established the presence of a magnetosphere at Mercury that is Earth-like in nature, though much smaller both in absolute terms and in proportion to the size of the planet (Ness et al., 1974, 1975, 1976; Russell et al., 1988; Slavin, 2004). These initial flybys revealed the presence of signatures of bursty magnetic reconnection between the interplanetary and planetary magnetic fields (Russell and Walker, 1985), which are called flux transfer events (FTEs) and which had previously been observed at Earth (Russell and Elphic, 1978; Russell and Elphic, 1979). Subsequently, the Hermean magnetosphere has been extensively sampled by the National Aeronautics and Space Administration MESSENGER (MErcury Surface, Space ENvironment, GEochemistry and Ranging) spacecraft, which orbited the planet between 2011 and 2015 (Anderson et al., 2008, 2011), demonstrating in particular that FTEs are commonplace at Mercury (Slavin et al., 2012).

Flux transfer events give rise to a characteristic bipolar signature in the component of the magnetic field normal to the local magnetopause surface,  $B_N$ , and an enhancement is observed in the field magnitude,  $|\mathbf{B}|$  (Russell and Elphic, 1978; Russell and Elphic, 1979; Elphic, 1995). The occurrence of FTEs at Mercury is found to exhibit the same interplanetary magnetic field (IMF) control as at Earth, with FTEs being preferentially observed for the southward IMF conditions that favor reconnection with the northward directed planetary field (Leyser et al., 2017). The high repetition rate and large relative size of FTEs at Mercury, in terms of magnetic flux content compared with the overall flux contained within the Hermean magnetosphere, mean that they are already thought to be the major driver of Mercury's magnetospheric dynamics (Slavin et al., 2008, 2009, 2010, 2012; Imber et al., 2014). Imber et al. (2014) carried out a survey of large

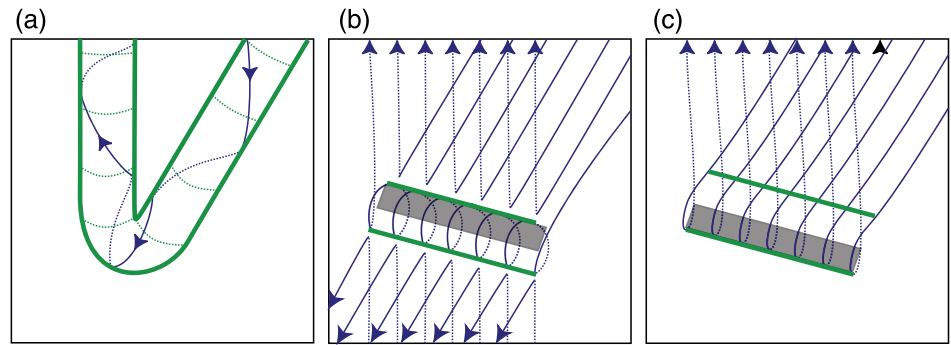


**Figure 1.** A cut-away illustration of the three main FTE mechanisms, reproduced from Fear et al. (2017). The panels show a view, from normal to the magnetopause plane, of the open field lines in (a) the Russell and Elphic (1978), flux tube model, (b) the Lee and Fu (1985) multiple X-line model, and (c) the Southwood et al. (1988)/Scholer (1988) single X-line model. The gray rectangles indicate the surfaces across which the magnetic flux is evaluated in equation (2).

FTEs observed in Mercury's magnetosheath (requiring the peak value of  $|\mathbf{B}|$  within the FTE to exceed the background magnetospheric magnetic field strength at the nearest magnetopause crossing); they estimated the mean flux content of a “large” FTE to be 0.06 MWb, with an extreme value of 0.22 MWb observed for one event. Since the size of Mercury's polar cap is estimated to be about 4–6 MWb (Alexeev et al., 2010), this would suggest that an individual FTE could open flux corresponding to  $\sim 1$ –5% of the open flux content of Mercury's magnetosphere. This compares with previous estimates, from spacecraft observations, of individual FTEs opening between 0.1–1% of Earth's polar cap (see summary by Fear et al., 2017). Factoring in the high repetition rate, Imber et al. (2014) concluded that FTEs could provide at least  $\sim 30\%$  of the flux transport needed to drive Mercury's substorm cycle, compared with less than 2% at Earth.

However, the numbers quoted above all originate from calculations based on spacecraft observations. Studies using data from ionospheric radars at Earth have suggested that FTE flux content could be up to an order of magnitude higher than commonly calculated, with individual terrestrial FTEs potentially opening  $\sim 10\%$  of the polar cap (Lockwood et al., 1990; Milan et al., 2000). Fear et al. (2008, 2017) argued that this discrepancy could be due to implicit assumptions that are made when analyzing the spacecraft data. In order to understand these assumptions, it is necessary to review the three different reconnection-based mechanisms that have been proposed to explain the observed  $B_N$  and  $|\mathbf{B}|$  signatures, which are sketched in Figure 1 and discussed further in section 2 of Fear et al. (2008). In the first, a flux tube forms as a result of a pulse of reconnection at a longitudinally narrow reconnection site (Russell and Elphic, 1978, 1979); in the second, a flux rope forms between a pair of (potentially extended) parallel reconnection lines, or X-lines (Lee and Fu, 1985); in the third, the signatures arise as a result of a “bulge” in the magnetopause boundary layer which is formed by a pulse in the reconnection rate at a single, but also potentially extended, X-line (Southwood et al., 1988; Scholer, 1988). The normal procedure employed by spacecraft studies is to estimate the cross-sectional area of the flux rope, and then calculate the total amount of flux mapping through that cross section:

$$\Phi_{\text{rope}} = B_{\text{axial}} \pi r^2 \quad (1)$$

where  $B_{\text{axial}}$  is the component of the magnetic field strength parallel to the axis of the flux rope, and  $r$  is the flux rope radius. Fear et al. (2017) argue that this calculation tacitly assumes the Russell and Elphic (1978, 1979) scenario, as it is only in this mechanism that  $\Phi_{\text{rope}}$  is representative of the total amount of magnetic flux opened in the burst of reconnection. In the Lee and Fu (1985) multiple X-line scenario, it is important to distinguish between the “flux transfer event” (in the sense of the reconnection burst as a whole) and the flux rope; the burst of reconnection gives rise to the flux rope observed by the spacecraft, but in doing so opens a potentially much greater amount of magnetic flux which does not map through the flux rope, but does map to the ionosphere (see Figure 1b). In the multiple X-line scenario, calculating  $\Phi_{\text{rope}}$  quantifies the open flux which maps through the flux rope, but neglects the (potentially much greater) amount of magnetic flux that is opened in the formation of the flux rope. Furthermore, in the Southwood et al. (1988)/Scholer (1988) single X-line scenario, the structure which gives rise to the in situ signatures is not a flux rope, and hence calculating  $\Phi_{\text{rope}}$  is not appropriate. Instead, Fear et al. (2017) argue that for either of the latter two (longer

X-line) scenarios, the total amount of magnetic flux opened in a burst of reconnection is more completely represented by the flux which maps through the gray surfaces in Figure 1, that is,

$$\Phi_{\text{total}} = B_N r L \quad (2)$$

where  $B_N$  is, as above, the component of the magnetic field within the FTE that is normal to the magnetopause,  $r$  is again the FTE radius and  $L$  is the length of the reconnection line (and hence the FTE) at the magnetopause. Fear et al. (2017) examined two case studies for which they reported simultaneous observation of in situ signatures of FTEs at Earth's magnetopause and their ionospheric counterpart in radar data. They compared the fluxes  $\Phi_{\text{rope}}$  and  $\Phi_{\text{total}}$  calculated from equations (1) and (2) with estimates of FTE flux content inferred directly from the ionospheric signatures. In the first case, the spacecraft was separated by several hours of magnetic local time from the location at which the ionospheric signatures were observed. The local time separation between the in situ signatures observed by the spacecraft at the magnetopause and the ionospheric signatures was used to infer the reconnection line (and FTE) length,  $L$ .  $\Phi_{\text{rope}}$  was found to be nearly 2 orders of magnitude smaller than the ionospheric estimate, but  $\Phi_{\text{total}}$  and the ionospheric estimate were consistent within error bars. In the second example, the spacecraft and ionospheric observations were in the same local time sector; this removed information on the X-line length, but a closer one-to-one mapping was found between the spacecraft and ionospheric signatures. Given the lack of information on the total extent of the X-line,  $\Phi_{\text{total}}$  and the ionospheric estimates were evaluated assuming an X-line length of 2.7 hr of MLT, corresponding to the extent across which the radar signatures were observed. Within this local time sector, the ionospheric estimate and  $\Phi_{\text{total}}$  were found to be consistent.

In this paper, we explore the implications for flux transfer by FTEs at Mercury's magnetosphere if longer X-line mechanisms are explicitly considered. Our purpose in doing so is twofold. First, if the arguments put forward by Fear et al. (2017) are valid, they apply equally to Mercury and could indicate that the global contribution of FTEs to Mercury's global convection cycle have been underestimated (even though they are already thought to dominate). If that is the case, it would then follow that FTEs could provide a higher proportion of the flux transport needed to drive Mercury's substorm cycle. Second, Mercury provides a useful test of those arguments; a naive scaling up from the discrepancy at Earth (0.1–1% versus 10% of the polar cap being opened in one burst) to Mercury (where up to 5% of the polar cap is already thought to be opened in an individual large burst) could easily lead to FTE sizes that are unfeasibly large. Therefore, quantifying reasonable upper bounds for  $\Phi_{\text{total}}$  at Mercury provides a useful test of the arguments made by Fear et al. (2017) at Earth.

## 2. Results

In order to evaluate  $\Phi_{\text{total}}$  (equation (2)), we need to evaluate the three parameters  $L$ ,  $B_N$ , and  $r$ . We consider each of these parameters in turn. As discussed below, there are different extents to which we can constrain upper limits on these three parameters; for example, the typical length of the reconnection line at Mercury is not well constrained. We therefore aim to place a “sensible” upper limit on  $\Phi_{\text{total}}$ , rather than a hard upper value.

### 2.1. X-Line Length $L$

Fear et al. (2017) determined  $L$  by comparison between spacecraft and ionospheric observations. Here, we are only able to put a sensible upper limit on  $L$ , which we do by assuming that, as an upper extreme, reconnection may take place across the whole dayside magnetosphere along an X-line stretching from terminator to terminator (i.e., 12 hr of MLT). It may be that a reconnection line could extend further, by extending onto the postterminator flank magnetopause as has been observed (rarely) at Earth (Phan et al., 2006). In terms of inferences from MESSENGER observations, we can draw conflicting conclusions. Leyser et al. (2017) reported that, despite fairly uniform coverage of magnetopause crossings through dayside magnetic local times, most FTEs were observed within 3 hr of MLT from noon, which suggests that a maximum typical X-line length may be <6 hr of MLT. On the other hand, DiBraccio et al. (2013) surveyed magnetopause crossings for rotational discontinuities and found the magnetopause was open on crossings between 8 and 16 hr local time. While these magnetopause crossings were observed individually across many orbits, the fact that rotational discontinuities were prevalent suggests that a coherent X-line of 8 hr in MLT or above could be reasonable. In reality, the instantaneous X-line length is not well constrained; we proceed on the basis of a sensible upper limit of 12 hr but consider the scaling introduced by smaller values of  $L$  later.

We convert our X-line length, in terms of hours of MLT, into a value of  $L$  in kilometers by tracing along the magnetopause surface in an empirical model of magnetopause location, from 6 to 18 MLT. The model we choose is the Winslow et al. (2013) model, which follows the same functional form as the Shue et al. (1998) model used by Fear et al. (2017), but is adapted for Mercury. We assume a subsolar magnetopause stand-off distance of  $1.45 R_M$  and a flaring parameter  $\alpha$  of 0.5, which correspond to the midpoint values from Table 1 of Winslow et al. (2013). Tracing along this model magnetopause, with the reconnection line centered on the subsolar point, gives an upper limit estimate of  $L = 13,000$  km ( $5.3 R_M$ ).

## 2.2. Normal Flux Perturbation $B_N$

The second parameter that needs to be assessed is the normal perturbation to the magnetic field,  $B_N$ . Fear et al. (2017) noted that, strictly speaking, the correct value of  $B_N$  to use was the normal component of the magnetic field observed by a spacecraft that crosses through the center of the FTE, perfectly tangential to the surrounding magnetopause surface. In reality, most FTE crossings will pass further from the center of the FTE, as indicated by the impact parameter in force-free fitting (e.g. Slavin et al., 2010); therefore Fear et al. (2017) used the peak value of  $|B_N|$  observed in each case study. Here, we will do the same, but we will also consider extreme events in the reported literature. To our knowledge, the largest FTE signatures reported at Mercury (in terms of  $B_N$  deflection) occurred on 23 November 2011, which corresponded to a period of extreme solar wind driving due to the passage of a coronal mass ejection (Slavin et al., 2014). Peak-to-peak  $B_N$  perturbations of  $\sim 300$  nT were reported, and so we take an upper limit of  $|B_N|$  to be 150 nT. However, we will also consider the effect of a more ‘typical’ value of 25 nT (e.g. Russell and Walker, 1985; Slavin et al., 2012) later.

## 2.3. FTE Radius $r$

To estimate the flux rope radius  $r$ , we return to the survey carried out by Imber et al. (2014), who reported a mean FTE duration of 2.5 s, with a range of 0–8 s, noting that this range was comparable with typical FTE durations during MESSENGER’s first two Mercury flybys (Slavin et al., 2010). The mean duration reported by Imber et al. (2014) was slightly higher than the mean of 1.7 s reported from an “FTE shower” of 163 FTEs observed on one magnetopause crossing (Slavin et al., 2012); Imber et al. (2014) noted that this difference might be due to their more conservative selection criteria (requiring a peak  $|B|$  that exceeded the nearest-observed magnetospheric value) which may have biased their events toward longer durations. However, such a bias is compatible with the aims of the present study, to infer an upper limit on  $\Phi_{\text{total}}$ .

In order to convert these FTE durations into a radius  $r$ , we need to assume a typical propagation speed for FTEs at Mercury. The speed of FTEs at Mercury cannot be measured directly, as the Fast Imaging Plasma Spectrometer sensor of the Energetic Particle and Plasma Spectrometer on MESSENGER has a minimum integration time of 5 s (Andrews et al., 2007), which is longer than a typical FTE. We therefore follow Imber et al. (2014) and assume a typical speed of 400 km/s (based on typical magnetosheath Alfvén speeds during periods surrounding FTEs in their study), noting that Imber et al. (2014) cautioned that this might underestimate the actual velocity (and hence flux content). Combining this speed with the mean and upper FTE durations (2.5 and 8 s) reported by Imber et al. (2014) gives flux rope radii of 500 and 1,600 km ( $0.2$  and  $0.65 R_M$ ).

The aim of this study is to derive a “sensible” upper limit, and we are using upper extremes for both  $L$  and  $B_N$ . It is unlikely that on a given event an FTE will have extreme values for all three parameters  $L$ ,  $B_N$ , and  $r$ , and so for the purposes of calculating our “sensible upper limit” for  $\Phi_{\text{total}}$  we will use mean value of  $r = 500$  km. However, we will consider the impact of the upper extreme value of  $r = 1,600$  km later.

## 2.4. Total Flux $\Phi_{\text{total}}$

Multiplying the three parameters above ( $L = 13,000$  km,  $r = 500$  km,  $B_N = 150$  nT) results in an estimate of  $\Phi_{\text{total}}$  of just under 1 MWb. This compares with estimates of the mean value of  $\Phi_{\text{rope}}$  for large FTEs at Mercury of 0.06 MWb, and an extreme example of 0.2 MWb (Imber et al., 2014). It is also of interest to compare this value of  $\Phi_{\text{total}}$  with estimates of the polar cap size (i.e., the total amount of open flux in Mercury’s magnetosphere), which is estimated to be 4–6 MWb (Alexeev et al., 2010) based on modeling of Mercury’s magnetosphere fitted with data from Mariner 10 and early MESSENGER flybys. In doing so, we can make two points. First, our estimates for the upper limit on the total amount of flux opened by a single burst of magnetic reconnection at Mercury’s magnetopause are higher than the previously thought upper limit (which considers only the magnetic flux mapping through the FTE flux rope, and not the flux opened in the creation of the rope itself) by a factor of 5. Second, our estimates suggest that a large FTE at Mercury could

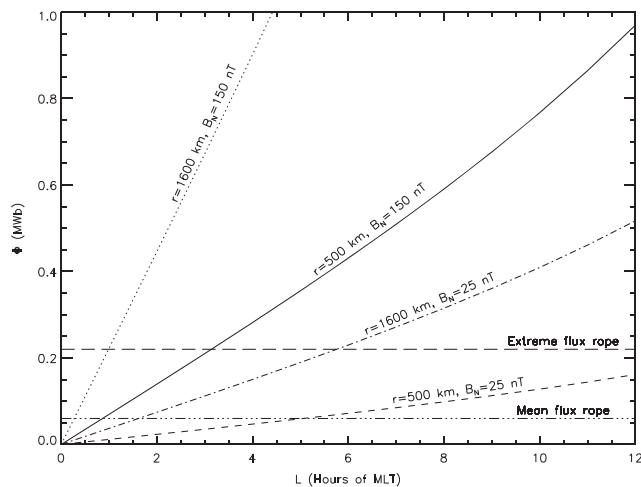


**Figure 2.** Dependence of the magnetic flux content  $\Phi$  on various assumptions. The four curves inclined to the horizontal show the dependence of  $\Phi_{\text{total}}$  on X-line length  $L$  for different assumptions about  $r$  and  $B_N$ , as labeled. The two horizontal lines (long-dash and long-dash-dot) show the extreme and mean values of  $\Phi_{\text{rope}}$  reported by Imber et al. (2014).

open approximately 15–25% of the polar cap—or equivalently, 4–6 large FTEs could cause the polar cap to double in size or (if matched by an equal amount of nightside reconnection) entirely refresh the polar cap.

### 3. Discussion

In this study, we have extended previous work (Fear et al., 2017) to consideration of bursty reconnection at Mercury's magnetopause, and evaluated a sensible upper limit for the contribution that FTEs can make to the global driving of Mercury's magnetosphere if extended X-line mechanisms for FTE generation are explicitly considered. In doing so, we make an important distinction between a flux transfer event (which we take to be a burst of magnetopause reconnection, which gives rise to a flux rope that can be detected by a spacecraft) and the flux rope itself. By evaluating  $\Phi_{\text{total}}$  (equation (2)), we place an approximate upper limit on the total amount of magnetic flux which an individual burst of magnetopause reconnection could contribute to Mercury's Dungey cycle, based on previously observed parameters. In doing so, we explicitly assume either the generation of FTEs by bursty reconnection at a single X-line (Southwood et al., 1988; Scholer, 1988) or by multiple X-lines (Lee and Fu, 1985), but we do not make an assumption about which of the two applies, since either mechanism will open the magnetic flux given by  $\Phi_{\text{total}}$  (Fear et al., 2017).

Of the three parameters required to evaluate  $\Phi_{\text{total}}$ ,  $B_N$  is an upper limit in the sense of it being our largest reported observation to date;  $L$  is a reasonable upper limit in that we have assumed the upper limit for the reconnection line length to be across the entire dayside magnetopause from 6 to 18 MLT (though it could in principle extend further), and  $r$  is a mean value, but one determined from a sample that was predisposed to larger events.  $\Phi_{\text{total}}$  scales linearly with all three of these parameters; hence, the total flux opened by an individual burst of magnetic reconnection could be greater than that calculated in section 2.4 if the radius ( $r$ ) of the FTE was at the larger end of the distribution observed by Imber et al. (2014) (assuming the other two parameters  $L$  and  $B_N$  are as we assumed), or equivalently if the FTE velocity used in this study and by Imber et al. (2014) is underestimated. Conversely,  $\Phi_{\text{total}}$  could be considerably smaller if the reconnection line extent was much smaller. As discussed above, statistics of FTE locations at Mercury are perhaps suggestive of an upper limit for a coherent X-line being below  $\sim 6$  hr of MLT (Leyser et al., 2017), though the presence of rotational discontinuities across a wider local time range might suggest the possibility of a longer coherent X-line (DiBraccio et al., 2013).

The effects of changing the three parameters  $L$ ,  $r$ , and  $B_N$  are shown in Figure 2, which shows the magnetic flux content  $\Phi$  as a function of  $L$  (in hours of magnetic local time). The four curves inclined to the horizontal show the dependence of  $\Phi_{\text{total}}$  (as evaluated from equation (2)) for different assumptions about  $r$  and  $B_N$ . These four curves are not quite straight lines; although  $\Phi$  increases linearly for small values of  $L$  due to the approximately circular shape of the Winslow et al. (2013) model near noon MLT, beyond about  $L = 8$  hr, the X-line length in kilometers starts to increase at a slightly faster rate in terms of hours of MLT due to the paraboloid shape of the magnetopause and hence  $\Phi$  also increases slightly more rapidly. (For simplicity, the X-line is assumed to be centered on the subsolar point in all cases.) The two horizontal lines represent  $\Phi_{\text{rope}}$  for the mean and extreme values determined by Imber et al. (2014). These values do not depend upon  $L$  and are equivalent to equation (1), but determined from a force-free fit.

The flux content under the assumptions discussed above ( $r = 500$  km,  $B_N = 150$  nT) is shown by the solid line in Figure 2. As noted above, if the X-line extends across the whole dayside face of the magnetopause, then  $\Phi_{\text{total}}$  is just under 1 MWb. However, if an X-line length of  $\sim 3$  hr of MLT is assumed, this would correspond to an FTE size roughly comparable with previous upper estimates (e.g. Imber et al., 2014), and an X-line length of  $\sim 1$  hr results in a flux content that is approximately equal to the mean flux rope flux content from Imber et al. (2014). Although we have regarded the solid line as a “sensible upper limit” based on the extreme value of  $B_N$ , the effect of using an upper limit value for  $r$  (1600 km; based on the upper end



of the duration range reported by Imber et al., 2014) is indicated by the dotted line. Changing this assumption increases the flux content by a factor of 3.2; a flux content of 1 MWb is obtained for an X-line length of  $\sim 4.5$  hr of MLT, comparable to the length we might infer from the FTE statistics reported by Leyser et al. (2017), and values of  $\Phi_{\text{total}}$  equivalent to the mean and extreme values of  $\Phi_{\text{rope}}$  reported by Imber et al. (2014) are obtained for X-line lengths of  $\sim 0.25$  and 1 hr of MLT, respectively.

The fluxes obtained assuming a more moderate and typical  $B_N$  peak perturbation of 25 nT are shown by the dashed and dash-dotted lines, which assume the mean and extreme flux rope radii of 500 and 1,600 km, respectively. Assuming the mean flux rope radius, a value of  $\Phi_{\text{total}}$  that is larger than the previously-reported mean value of  $\Phi_{\text{rope}}$  is obtained for X-line lengths that are greater than  $\sim 5$  hr of MLT. However, the value of  $\Phi_{\text{total}}$  obtained for a moderate  $B_N$  perturbation (25 nT) but an extreme radius (1,600 km) is approximately half of that for our original parameters ( $r = 500$  km,  $B_N = 150$  nT—solid line). Therefore, for these parameters, an X-line length of 12 hr results in just over 0.5 MWb of flux being opened, and any X-line longer than  $\sim 5.5$  hr results in a flux contribution that is greater than the extreme value of  $\Phi_{\text{rope}}$  calculated by Imber et al. (2014). When considering the three curves (solid, dotted, and dash-dotted) which represent cases where at least one of the parameters is at its upper limit, then  $\Phi_{\text{rope}}$  is a distinct underestimate for  $\Phi_{\text{total}}$  if the X-line length is above  $\sim 1$ –6 hr of MLT (depending on the parameter combination chosen).

Overall, if reconnection is free on occasion to extend across the full extent of Mercury's dayside magnetopause, then our results suggest that one large FTE could open magnetic flux equivalent to a sixth to a quarter of the typical size of Mercury's polar cap, rather than  $\sim 5\%$ . In other words, approximately 4–6 large FTEs could be all that is needed to refresh Mercury's polar cap entirely, if matched by an equivalent amount of nightside reconnection. This result has interesting implications for the balance of quasi-steady versus bursty reconnection in Mercury's magnetospheric system. Imber et al. (2014) estimated that FTEs could provide approximately 30% of the flux transport needed to drive Mercury's substorm cycle, based on the fact that the loading phase of substorms at Mercury is thought to last  $\sim 90$  s, and a conservative estimate that the tail magnetic flux content increases by  $\sim 1$  MWb in this time. Assuming the average magnetic flux content of an FTE to be 0.03 MWb (half of their average value for "large" FTEs), Imber et al. (2014) calculated that at a repetition rate of one FTE every 10 s, FTEs could transport 0.3 MWb during the growth phase of a substorm. The remaining 70% of the flux transport would therefore arise from quasi-steady reconnection. If we take our upper estimate for the total magnetic flux opened by an FTE, then FTEs are more than capable of providing the 1 MWb of flux in 90 s necessary to drive Mercury's substorm cycle. Based on the numbers above (i.e., the solid line in Figure 2), one large FTE extending across the full dayside magnetopause could open 1 MWb; perhaps more realistically, the 10 FTEs expected to occur during a typical substorm loading period could between them provide the 1 MWb necessary if they had the extreme values of  $B_N$  reported by Slavin et al. (2014), the average  $r$  for large FTEs reported by Imber et al. (2014) and if the reconnection site length  $L$  was  $\sim 1.5$  hr of MLT (solid line in Figure 2). Alternatively, those 10 FTEs could transfer the necessary 1 MWb of flux with a more typical  $B_N$  perturbation of 25 nT but a large radius of 1,600 km and an X-line length of 3 hours of MLT (dash-dotted line in Figure 2).

Imber et al. (2014) compared their substorm flux transport estimate with Earth, where based on a growth phase of 48 min (Partamies et al., 2013), 1 MWb FTEs occurring with a mean inter-event period of 8 min (Lockwood and Wild, 1993) could open  $\sim 6$  MWb of flux, corresponding to 2% of the 0.3 GWb of magnetic flux that is closed in a typical substorm (Milan et al., 2007), whereas based on ionospheric observations at Earth, Lockwood et al. (1990) and Milan et al. (2000) have estimated that individual, large FTEs can provide 30–100% of the total transpolar voltage. Based on the total flux contents of  $\sim 45$ –75 MWb estimated from both spacecraft and ionospheric observations by Fear et al. (2017), FTEs occurring at the same rate could be expected to open  $\sim 270$ –450 MWb during a growth phase, which is comparable with the amount of flux closed in a terrestrial substorm (Milan et al., 2007). Therefore, it appears that at both Mercury and Earth, FTEs may be capable of providing enough flux transport to drive the Dungey cycle both in its steady and time-varying states (i.e., the substorm cycle).

Recently, Slavin et al. (2019) reported four "Disappearing Dayside Magnetosphere" events, in which the MESSENGER spacecraft did not encounter the dayside magnetopause until it was at extremely high latitudes, despite the fact that the spacecraft reached altitudes below 300 km. These events were characterized by extremely high solar wind dynamic pressure, and intense southward IMF. The authors concluded that the disappearance of the dayside magnetosphere was due to solar wind compression and/or erosion of the

magnetosphere due to a high rate of dayside reconnection, though it was difficult to determine the relative contribution of these two effects. If the reconnection line is free, under extreme conditions, to extend over a significant part of Mercury's dayside magnetopause, then our results imply that FTEs could sometimes cause the disappearance of Mercury's dayside magnetosphere.

Finally, we note that of the three parameters in equation (2), the X-line length  $L$  is currently the least well constrained. The two-spacecraft BepiColombo mission will hopefully help to constrain this parameter further, both for regular Hermean conditions and extreme events such as those reported by Slavin et al. (2019).

#### 4. Conclusions

We have applied arguments from a recent study into the flux content of flux transfer events at Earth (Fear et al., 2017) to Mercury's magnetosphere. Using a statistically-determined mean flux rope radius for "large" Hermean FTEs (Imber et al., 2014), upper values for the magnetic perturbation due to the passage of the FTE flux rope as reported during a period of extreme solar wind driving at Mercury (Slavin et al., 2014) and making the assumption that, at its largest extent, the reconnection process could occur coherently along a single reconnection line across the entire dayside magnetosphere (12 hr in magnetic local time), we place a sensible upper limit for the total flux content of a large flux transfer event at Mercury to be  $\sim 1$  MWb. This value accounts for all of the magnetic flux that is opened in the burst of reconnection that results in the characteristic  $B_N$  signature observed by a spacecraft, not just the subset of flux which maps through the flux rope. This estimate is a factor of 5 greater than previous upper estimates of the flux content of FTEs at Mercury, which consider only the flux which maps through the flux rope itself (Imber et al., 2014). We emphasize that this is an upper limit, based largely on extreme values, but consideration of more moderate permutations results in flux estimates that are larger than previous upper limits. Furthermore, our calculations suggest that FTEs could be capable of providing enough flux transport to drive the substorm cycle at Mercury.

#### Acknowledgments

This work was primarily funded by the UK's Science and Technology Facilities Council (STFC) Ernest Rutherford Fellowship ST/K004298/2 (R. C. F.). R. C. F. and J. C. C. were also supported by STFC Consolidated Grant ST/R000719/1, and C. M. J. was supported by STFC Ernest Rutherford Fellowship ST/L004399/1. The data used in this study consist of numerical values quoted in the manuscript and from integrating along a path given by equation (2) of Winslow et al. (2013).

#### References

- Alexeev, I. I., Belenkaya, E. S., Slavin, J. A., Korth, H., Anderson, B. J., Baker, D. N., et al. (2010). Mercury's magnetospheric magnetic field after the first two MESSENGER flybys. *Icarus*, 209, 23–39. <https://doi.org/10.1016/j.icarus.2010.01.024>
- Anderson, B. J., Acuña, M. H., Korth, H., Purucker, M. E., Johnson, C. L., Slavin, J. A., et al. (2008). The structure of Mercury's magnetic field from MESSENGER's first flyby. *Science*, 321, 82–85. <https://doi.org/10.1126/science.1159081>
- Anderson, B. J., Johnson, C. L., Korth, H., Purucker, M. E., Winslow, R. M., Slavin, J. A., et al. (2011). The global magnetic field of Mercury from MESSENGER orbital observations. *Science*, 333, 1859–1862. <https://doi.org/10.1126/science.1211001>
- Andrews, G. B., Zurbuchen, T. H., Mauk, B. H., Malcom, H., Fisk, L. A., Gloeckler, G., et al. (2007). The energetic particle and plasma spectrometer instrument on the MESSENGER spacecraft. *Space Science Reviews*, 131, 523–556. <https://doi.org/10.1007/s11214-007-9272-5>
- DiBraccio, G. A., Slavin, J. A., Boardsen, S. A., Anderson, B. J., Korth, H., Zurbuchen, T. H., et al. (2013). MESSENGER observations of magnetopause structure and dynamics at Mercury. *Journal of Geophysical Research: Space Physics*, 118, 997–1008. <https://doi.org/10.1002/jgra.50123>
- Elphic, R. C. (1995). Observations of flux transfer events: A review. In P. Song, B. U. Sonnerup, & M. F. Thomsen (Eds.), *Physics of the magnetopause* (pp. 225–233). Washington D. C.: American Geophysical Union. <https://doi.org/10.1029/GM090p0225>
- Fear, R. C., Milan, S. E., Fazakerley, A. N., Lucek, E. A., Cowley, S. W. H., & Dandouras, I. (2008). The azimuthal extent of three flux transfer events. *Annales Geophysicae*, 26, 2353–2369. <https://doi.org/10.5194/angeo-26-2353-2008>
- Fear, R. C., Trenchi, L., Coxon, J. C., & Milan, S. E. (2017). How much flux does a flux transfer event transfer? *Journal of Geophysical Research: Space Physics*, 122, 12,310–12,327. <https://doi.org/10.1002/2017JA024730>
- Imber, S. M., Slavin, J. A., Boardsen, S. A., Anderson, B. J., Korth, H., McNutt, R. L., & Solomon, S. C. (2014). MESSENGER observations of large dayside flux transfer events: Do they drive Mercury's substorm cycle? *Journal of Geophysical Research: Space Physics*, 119, 5613–5623. <https://doi.org/10.1002/2014JA019884>
- Lee, L. C., & Fu, Z. F. (1985). A theory of magnetic flux transfer at the Earth's magnetopause. *Geophysical Research Letters*, 12, 105–108. <https://doi.org/10.1029/GL012i002p00105>
- Leyser, R. P., Imber, S. M., Milan, S. E., & Slavin, J. A. (2017). The influence of IMF clock angle on dayside flux transfer events at Mercury. *Geophysical Research Letters*, 44, 10,829–10,837. <https://doi.org/10.1002/2017GL074858>
- Lockwood, M., Cowley, S. W. H., Sandholt, P. E., & Lepping, R. P. (1990). The ionospheric signatures of flux transfer events and solar wind dynamic pressure changes. *Journal of Geophysical Research*, 95, 17,113–17,135. <https://doi.org/10.1029/JA095iA10p17113>
- Lockwood, M., & Wild, M. N. (1993). On the quasi-periodic nature of magnetopause flux transfer events. *Journal of Geophysical Research*, 98, 5935–5940. <https://doi.org/10.1029/92JA02375>
- Milan, S. E., Lester, M., Cowley, S. W. H., & Brittnacher, M. (2000). Convection and auroral response to a southward turning of the IMF: Polar UVI, CUTLASS, and IMAGE signatures of transient magnetic flux transfer at the magnetopause. *Journal of Geophysical Research*, 105, 15,741–15,755. <https://doi.org/10.1029/2000JA900022>
- Milan, S. E., Provan, G., & Hubert, B. (2007). Magnetic flux transport in the Dungey cycle: A survey of dayside and nightside reconnection rates. *Journal of Geophysical Research*, 112, A01209. <https://doi.org/10.1029/2006JA011642>

- Ness, N. F., Behannon, K. W., Lepping, R. P., & Whang, Y. C. (1975). The magnetic field of Mercury, 1. *Journal of Geophysical Research*, 80, 2708–2716. <https://doi.org/10.1029/JA080i019p02708>
- Ness, N. F., Behannon, K. W., Lepping, R. P., & Whang, Y. C. (1976). Observations of Mercury's magnetic field. *Icarus*, 28, 479–488. [https://doi.org/10.1016/0019-1035\(76\)90121-4](https://doi.org/10.1016/0019-1035(76)90121-4)
- Ness, N. F., Behannon, K. W., Lepping, R. P., Whang, Y. C., & Schatten, K. H. (1974). Magnetic field observations near Mercury: Preliminary results from Mariner 10. *Science*, 185(4146), 151–160. <https://doi.org/10.1126/science.185.4146.151>
- Partamies, N., Juusola, L., Tanskanen, E., & Kauristie, K. (2013). Statistical properties of substorms during different storm and solar cycle phases. *Annales Geophysicae*, 31, 349–358. <https://doi.org/10.5194/angeo-31-349-2013>
- Phan, T. D., Hasegawa, H., Fujimoto, M., Oieroset, M., Mukai, T., Lin, R. P., & Paterson, W. (2006). Simultaneous Geotail and Wind observations of reconnection at the subsolar and tail flank magnetopause. *Geophysical Research Letters*, 33, L09104. <https://doi.org/10.1029/2006GL025756>
- Russell, C. T., Baker, D. N., & Slavin, J. A. (1988). The magnetosphere of Mercury. In C. Chapman (Ed.), *Mercury* (pp. 514–561). Tucson: University of Arizona Press.
- Russell, C. T., & Elphic, R. C. (1978). Initial ISEE magnetometer results: Magnetopause observations. *Space Science Reviews*, 22, 681–715. <https://doi.org/10.1007/BF00212619>
- Russell, C. T., & Elphic, R. C. (1979). ISEE observations of flux transfer events at the dayside magnetopause. *Geophysical Research Letters*, 6, 33–36. <https://doi.org/10.1029/GL006i001p00033>
- Russell, C. T., & Walker, R. J. (1985). Flux transfer events at Mercury. *Journal of Geophysical Research*, 90, 11,067–11,074. <https://doi.org/10.1029/JA090iA11p11067>
- Scholer, M. (1988). Magnetic flux transfer at the magnetopause based on single X line bursty reconnection. *Geophysical Research Letters*, 15, 291–294. <https://doi.org/10.1029/GL015i004p00291>
- Shue, J.-H., Song, P., Russell, C. T., Steinberg, J. T., Chao, J. K., Zastenker, G., et al. (1998). Magnetopause location under extreme solar wind conditions. *Journal of Geophysical Research*, 103, 17,691–17,700. <https://doi.org/10.1029/98JA01103>
- Slavin, J. A. (2004). Mercury's magnetosphere. *Advances in Space Research*, 33, 1859–1874. <https://doi.org/10.1016/j.asr.2003.02.019>
- Slavin, J. A., Acuña, M. H., Anderson, B. J., Baker, D. N., Benna, M., Boardsen, S. A., et al. (2009). MESSENGER observations of magnetic reconnection in Mercury's magnetosphere. *Science*, 324, 606–610. <https://doi.org/10.1126/science.1172011>
- Slavin, J. A., Acuña, M. H., Anderson, B. J., Baker, D. N., Benna, M., Gloeckler, G., et al. (2008). Mercury's magnetosphere after MESSENGER's first flyby. *Science*, 321, 85–89. <https://doi.org/10.1126/science.1159040>
- Slavin, J. A., DiBraccio, G. A., Gershman, D. J., Imber, S. M., Poh, G. K., Raines, J. M., et al. (2014). MESSENGER observations of Mercury's dayside magnetosphere under extreme solar wind conditions. *Journal of Geophysical Research: Space Physics*, 119, 8087–8116. <https://doi.org/10.1002/2014JA020319>
- Slavin, J. A., Imber, S. M., Boardsen, S. A., DiBraccio, G. A., Sundberg, T., Sarantos, M., et al. (2012). MESSENGER observations of a flux-transfer-event shower at Mercury. *Journal of Geophysical Research*, 117, A00M06. <https://doi.org/10.1029/2012JA017926>
- Slavin, J. A., Lepping, R. P., Wu, C.-C., Anderson, B. J., Baker, D. N., Benna, M., et al. (2010). MESSENGER observations of large flux transfer events at Mercury. *Geophysical Research Letters*, 37, L02105. <https://doi.org/10.1029/2009GL041485>
- Slavin, J. A., Middleton, H. R., Raines, J. M., Jia, X., Zhong, J., Sun, W.-J., et al. (2019). MESSENGER observations of disappearing dayside magnetosphere events at Mercury. *Journal of Geophysical Research: Space Physics*, 124, 6613–6635. <https://doi.org/10.1029/2019ja026892>
- Southwood, D. J., Farrugia, C. J., & Saunders, M. A. (1988). What are flux transfer events? *Planetary and Space Science*, 36, 503–508. [https://doi.org/10.1016/0032-0633\(88\)90109-2](https://doi.org/10.1016/0032-0633(88)90109-2)
- Winslow, R. M., Anderson, B. J., Johnson, C. L., Slavin, J. A., Korth, H., Purucker, M. E., et al. (2013). Mercury's magnetopause and bow shock from MESSENGER magnetometer observations. *Journal of Geophysical Research: Space Physics*, 118, 2213–2227. <https://doi.org/10.1002/jgra.50237>